Supplementary of "Quantum ensemble learning with a programmable superconducting processor"

I. NUMERICAL SIMULATION

To demonstrate the efficiency of our Adaboost.Q algorithm, we compare it with the conventional Adaboost.M1 algorithm using numerical simulations. The Adaboost.M1 algorithm is shown in Algorithm S1. The classification task considered here is a ten-class classification task, which is the same one as considered in the main text and carried out with the same structure of the QNN circuit. Each ensemble classifier is composed of four base classifiers. We benchmark the accuracy of each algorithm for 500 times, with the initial trainable parameters randomly generated each time. The results are shown in Fig. 3d of the main text.

Algorithm S1 AdaBoost.M1

Input:

Training set $\mathcal{T} = \{(x_i, y_i)\}_{i=1}^{N}$, where $x_i \in \mathcal{X}$ and $y_i \in \mathcal{Y} \subseteq \{1, 2, ..., K\}$;
The number of weak classifier L;
A series of weak classifiers $\{G(x, \boldsymbol{\theta}_l)\}_{l=1}^{L}$,

$$G(x, \boldsymbol{\theta}_l) : \mathcal{X} \to \boldsymbol{R}^K, \quad G(x_i, \boldsymbol{\theta}_l) = \{P_k(x_i, \boldsymbol{\theta}_l)\}_{k=1}^{K},$$

with $P_k(x_i, \boldsymbol{\theta}_l)$ defined in the main text.

Output:

Combined classifier

$$\mathcal{G}(x) = \sum_{l=1}^{L} \alpha_l \cdot G(x, \boldsymbol{\theta}_l^*),$$

where α_l and $\boldsymbol{\theta}_l^*$ are the weight and optimal parameters of the lth classifier. The output label of the combined classifier is

$$\tilde{y}_i = \arg\max_k \mathcal{G}(x_i).$$

1: Initialize the weights of the training set,

$$\boldsymbol{w}_1 = \{w_{1,i}\}_{i=1}^{N},$$

where $w_{1,i} = 1/N$.

2: **for** $l = 1 : L$ **do**

3: Train the classifier $G(x, \boldsymbol{\theta})$ with the weighted training set. Obtain

$$\tilde{y}_{l,i} = \arg\max_k G(x_i, \boldsymbol{\theta}_l^*),$$

with error rate:

$$e_l = \sum_{i=1}^{N} w_{l,i}\, \delta(\tilde{y}_{l,i}, y_i).$$

4: Calculate the lth classifier's weight:

$$\alpha_l = \ln\left(\frac{1 - e_l}{e_l}\right) + \ln(K - 1).$$

5: Update the weight of training set:

$$w_{l+1,i} = \frac{w_{l,i}}{Z_{l+1}} \exp(\alpha_l \delta_{\tilde{y}_{l,i} y_i}),$$

with the normalization factor

$$Z_{l+1} = \sum_{i=1}^{N} w_{l,i} \exp(\alpha_l \delta_{\tilde{y}_{l,i} y_i}).$$

6: **end for**

II. EXPERIMENTAL INFORMATION

A. Device information

Our experiments are performed on a superconducting quantum processor, which has 11×11 transmon qubits aligned in a square grid, with the nearest neighboring qubits connected by tunable couplers [1]. Each qubit has individual microwave control for realizing single-qubit gates and flux control for frequency modulation. Each coupler has an individual flux control for tuning the coupling strength between the corresponding two neighboring qubits. As illustrated in Fig. 2 and Fig. 4 of the main text, we use two 10-qubit chains and a 15-qubit chain for realizing the quantum neural network (QNN) and the quantum convolutional neural network (QCNN) in our experiment, with their properties and gate errors shown in Fig. S1.

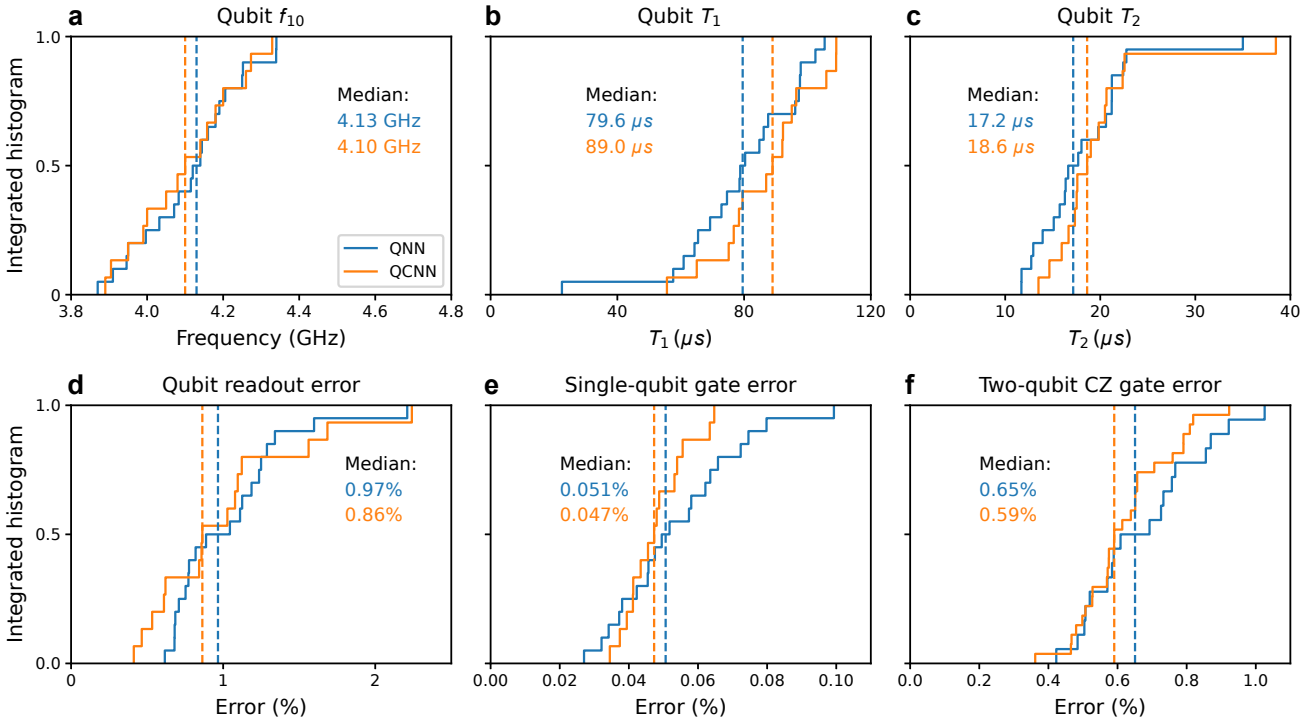

FIG. S1. **Integrated histograms of qubit parameters. a**, Qubit idle frequency. **b**, Qubit relaxation time measured at the idle frequency. **c**, Qubit dephasing time measured using Hahn echo sequence. **d**, Readout fidelity of the qubit. **e**, Pauli error of simultaneous single-qubit gate. **f**, Pauli error of two-qubit CZ gate. Dashed lines indicate the median values.

B. Quantum data preparation

For the quantum phase recognition task in the main text, we use variational quantum circuits (VQCs) to prepare the approximate ground states in the training and test sets. A general structure of the VQC is composed of blocks of single- and two-qubit gates. Each block contains six layers of parameterized single-qubit gates and two layers of two-qubit CZ gates, as shown in Fig. S3. We use three and four blocks to prepare the quantum states in the training and test sets, respectively. The circuit is implemented on the quantum processor before applying the QCNN circuit.

For a given model parameter set $\{h_1, h_2\}$, we determine the parameters in the VQC by minimizing the energy expectation value of the corresponding Hamiltonian in a classical computer by using the gradient-based Nadam optimizer. The variational parameters are initialized to be the optimized ones of the neighboring point if there existed one, otherwise with each element randomly generated in the range of $[-\pi, \pi)$. The optimization procedure ends when the energy value no longer decreases in the next 20 iteration steps. The circuit is accepted when 1). the energy differences between the neighboring steps is less than 5×10^{-5} for 20 iterations; 2). the difference between the optimized energy and the ideal ground state energy obtained by the DMRG (Density Matrix Renormalization Group) method is less than 0.5; and 3). the corresponding order parameters of the optimized states in each of the three phases meet the following criteria: a). $\langle S \rangle > 0.2$ for states in SPT phase; b). $\langle S \rangle < 0.2$

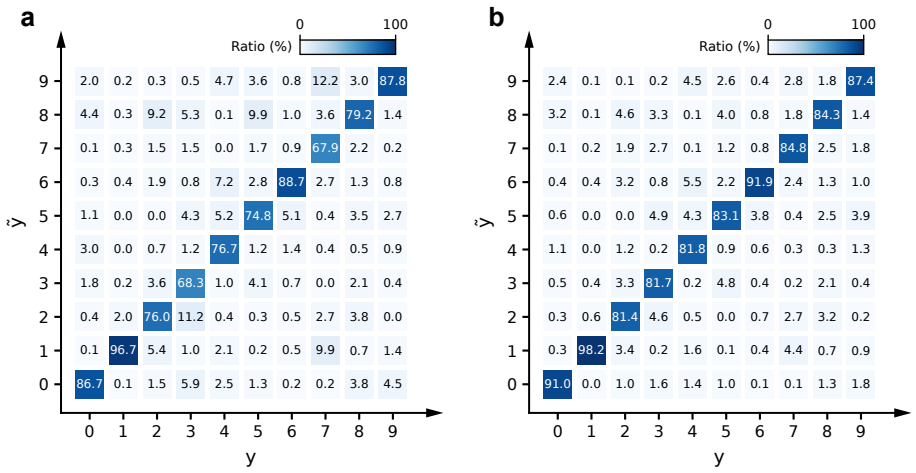

FIG. S2. **Comparison of detailed classification results between single classifier and ensemble classifier.** The classification performance of the trained model on the whole MNIST test set, where the ratios of classifying y to $\tilde{y}$ are displayed. **a**, Single classifier's classification result. **b**, Ensemble classifier's classification result.

and $\langle X_7 X_8 \rangle > 0$ for states in FM phase; and c). $\langle S \rangle < 0.2$ and $\langle X_7 X_8 \rangle < 0$ for states in Ising phase. If not accepted, the optimization will be retried with newly and randomly generated variational parameters. The model parameter sets that fail 10 retries will be discarded in this work, which usually locate around the critical points. The order parameters of the numerically obtained quantum states in the training and test sets are shown in Fig. S4. As a result, we obtain approximate ground states with their energies locating within the range of 1.8% above the ground state energies, as shown in Fig. S5.

C. More experimental data

The detailed classification results for single and ensemble classifiers on the MNIST hand-written digits dataset in the main text are displayed in Fig S2.

[1] S. Xu, Z.-Z. Sun, K. Wang, L. Xiang, Z. Bao, Z. Zhu, F. Shen, Z. Song, P. Zhang, W. Ren, *et al.*, Digital simulation of projective non-abelian anyons with 68 superconducting qubits, Chinese Physics Letters **40**, 060301 (2023).

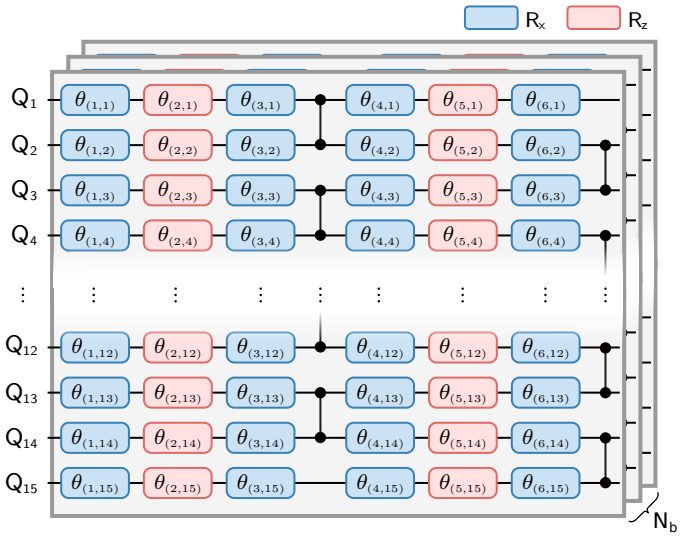

FIG. S3. **Varartional quantum circuit for preparing the quantum phase.** The circuit consists of N_b blocks, each of which is composed of six layers of single-qubit gates inserted by two layers of two-qubit CZ gates. The single-qubit gate rotation angles serve as variational parameters. The quantum states in the training and test sets are generated with block numbers $N_b = 3$ and 4, respectively.

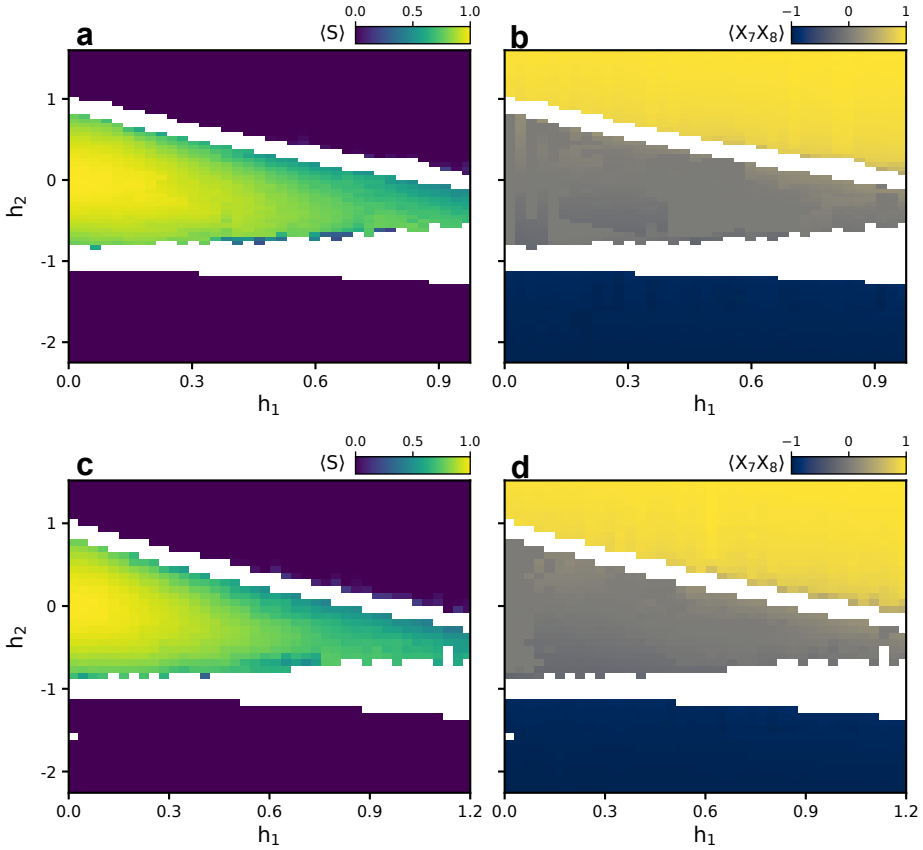

FIG. S4. $\langle S \rangle$ **and** $\langle X_7 X_8 \rangle$ **of quantum states generated by VQCs during the numerical simulation.** Expectation values of the observables S and $X_7 X_8$ of the quantum states in training and test set are shown in (a), (b) and (c), (d), respectively.

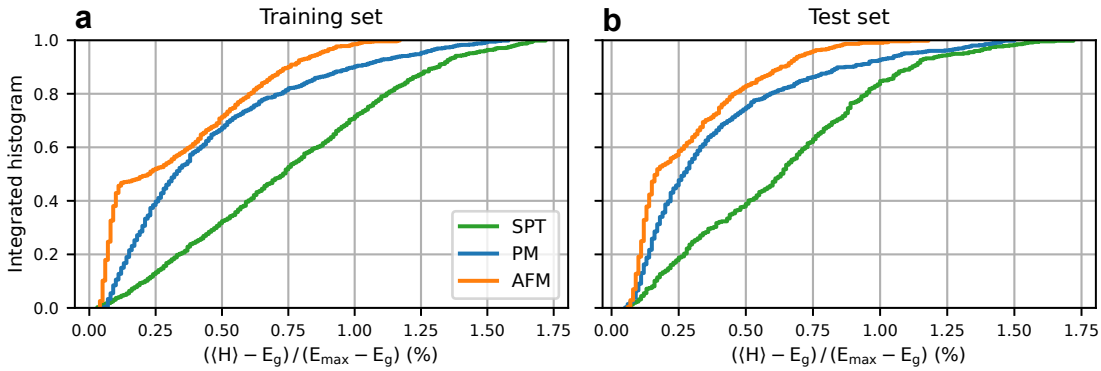

FIG. S5. **Integrated histograms of the energy deviation from the ground states for the variationally generated quantum states in the three phases.** Here $\langle H \rangle$, $E_{\max}$, and E_{g} represent the energy of the approximate ground states, the maximum eigen energy and the energy of the ideal ground states, respectively.